

## Activity expansion calculation of shock-compressed helium: The liquid Hugoniot

Marvin Ross, Forrest Rogers, Nicholas Winter, and Gilbert Collins  
Lawrence Livermore National Laboratory, Livermore, California 94551, USA

(Received 8 May 2007; published 10 July 2007)

The Hugoniot of shock-compressed liquid helium was calculated using the activity expansion dense plasma program. The predicted maximum compression is at 100 GPa and 58 000 K, at a density nearly six-fold that of the initial state. Comparisons are made with recent path-integral Monte Carlo simulations, which predict a smaller maximum compression of 5.24-fold, near 360 GPa and 150 000 K.

DOI: [10.1103/PhysRevB.76.020502](https://doi.org/10.1103/PhysRevB.76.020502)

PACS number(s): 67.60.-g, 62.50.+p, 64.10.+h, 64.30.+t

### I. INTRODUCTION

As helium is the second most abundant element in the universe, its equation of state (EOS) at astrophysical conditions is of great scientific interest. At the present time, only shock-wave experiments have access to these extreme pressures and temperatures, and the only shock-wave measurements for liquid helium, reported to date, are those of Nellis *et al.*,<sup>1</sup> made using the Livermore two-stage gas gun. The Hugoniot is the locus of states accessible by shock-compressing a sample starting from a set initial state. With liquid He, Nellis *et al.* obtained a maximum compression of  $V_0/V=3.3$ , at a pressure of 15.6 GPa, and a calculated temperature of 12 000 K.  $V_0$  is the initial volume of the liquid being shock compressed, and  $V$  is the volume at maximum compression. From the perspective of astrophysical modeling, an accurate knowledge of the maximum compression attained on the Hugoniot places an important constraint on a useful EOS model. In order to obtain an effective pair potential useful for theoretical modeling, Ross and Young (RY) employed a soft-sphere fluid theory and fitted the potential to the principal Hugoniot (single shock), and to a second or reflected shock near 56 GPa and 22 000 K.<sup>2</sup> Subsequently, Chabrier and co-workers<sup>3</sup> used liquid hard-sphere perturbation theory to obtain a potential from the Hugoniot measurements.

The chemical picture methods<sup>2,3</sup> are best suited to normal liquids, but at the extreme conditions reached in astrophysical applications they become increasingly unreliable due to  $\text{He}_2^+$  dimer formation, ion-ion scattering, and the treatment of electron excitation leading to the fully ionized plasma state. An advance in this direction was made recently by Militzer.<sup>4</sup> Using path-integral Monte Carlo (PIMC) and density functional theory–molecular dynamics (DFTMD) simulation methods to calculate the He Hugoniot, Militzer obtained a 5.24-fold maximum compression near 360 GPa and 150 000 K. With more powerful lasers,<sup>5</sup> helium can be shocked to pressures high enough to examine and help to develop a variety of potentially useful theoretical models. In this paper we report calculations of the He Hugoniot made using the activity expansion (ACTEX) dense plasma program. ACTEX predicts a 5.95-fold maximum compression near 100 GPa and 58 000 K. The method is described in Sec. II. The results of calculations are in Sec. III and they are discussed in Sec. IV.

### II. THEORY

Hugoniots are calculated from an equation of state by solving the equation

$$E - E_0 = (1/2)(P + P_0)(V_0 - V). \quad (1)$$

$E$ ,  $P$ , and  $V$  are the total energy, pressure, and volume of the final shocked state, respectively, and the subscripted variables refer to the initial conditions. For liquid He at 4.2 K,  $V_0=32.4 \text{ cm}^3/\text{mol}$ . The starting point for the ACTEX EOS program<sup>6–10</sup> are the Coulomb interactions between all the electrons and nuclei in the system, in bound, scattered, and free states. The non-ideal Helmholtz free energy is expanded in terms of two-body, three-body, etc., clusters, i.e., an Abe<sup>11</sup> cluster expansion.<sup>6,7</sup> The leading terms are

$$\frac{F - F_0}{VkT} = S_R + \sum_{i,j} S_{i,j} + \sum_{i,j,k} S_{i,j,k}, \quad (2)$$

$S_R=1/12\pi\lambda_D^3$ , where  $\lambda_D$  is the ion-ion Debye screening length, and the higher-order terms are

$$S_{i,j} = -n_i n_j \left[ B_{i,j}(T, \lambda_D) + 2\pi \int_0^\infty \left( \beta u_{i,j} - \frac{\beta u_{i,j}}{2} \right) r^2 dr \right],$$

and similarly for  $S_{i,j,k}$ , etc.

$B_{i,j}(T, \lambda_D)$  is the second virial coefficient for a mixture of ions and electrons in a static screened potential<sup>8,9</sup> and  $\beta = 1/kT$ . The  $u_{i,j}$ 's are the ion-ion, electron-electron, and electron-ion potentials. Electron-ion potentials were obtained for each electron shell by solving the Dirac equation iteratively, until a match with experimental ionization energies was obtained. The potentials were fitted to an analytic function.<sup>9</sup> The free energy is transformed into an activity expansion, in terms of a pressure,<sup>10</sup> that accounts for the formation of ions, atoms, and molecules. Quantum effects are introduced by replacing the Boltzmann factors  $e^{-\beta u}$  with a trace and using the method of Cooper and DeWitt<sup>12</sup> to introduce electron degeneracy. Consequently, thermal excitation and pressure ionization result naturally from the effect of multiparticle Coulomb interactions on bound states and without the introduction of *ad hoc* assertions. This is a definite advantage over the chemical picture methods in current use, which introduce *ad hoc* models to obtain these effects.

Equation (2) recovers the plasma strong-coupling limit when a sufficient number of terms are included.<sup>10</sup> However,

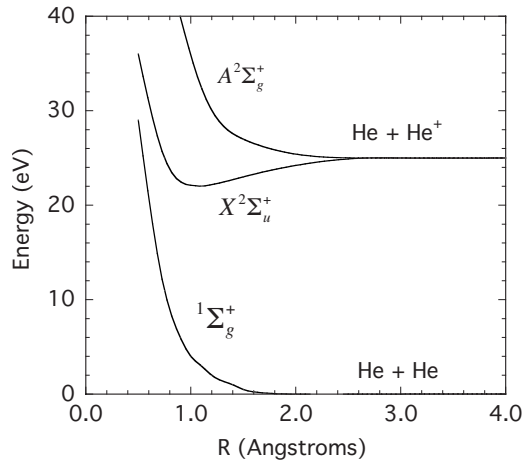


FIG. 1. Helium intermolecular potentials used in the ACTEX calculations.

at low temperature and high density plasma-neutral and neutral-neutral interactions become important. The Mayer activity expansion<sup>13</sup> has a very limited range of convergence for repulsive interactions. In order to include the effect of neutrals, we have developed an activity expansion method<sup>8</sup> that converges similarly to the virial expansion for repulsive neutral interactions. So far, we are only able to account for terms of order of the second virial correction. Consequently, the ACTEX method works best for partially ionized, low- to moderate-density plasmas, and for multiply ionized plasmas. This places a lower limit to the pressures that may be reliably predicted. In such cases, potential energy functions for He-He and He<sub>2</sub><sup>+</sup> need to be introduced.

In principle there are an infinite number of He-He\* excited states lying just below He<sub>2</sub><sup>+</sup> in energy that would produce a divergent partition function in the absence of many-body effects. These states make only a small contribution to the EOS.<sup>14</sup> In order to get an expansion that selects the relevant species at a given temperature, it is necessary to split the cluster coefficients into bound and scattering parts.<sup>6,10</sup> At the temperatures of interest herein, the rotovibrational and scattering states are nearly classical and were calculated in the WKB approximation.

The Hugoniot calculations reported here include potential energy curves calculated for the ground state and the lowest bound and scattered states of the He<sub>2</sub><sup>+</sup> system. Since the low-lying states have long been of importance to experimental and theoretical chemists, for studying the physics of He-He<sup>+</sup> scattering,<sup>15,16</sup> it is necessary to include these interactions in theoretical models analyzing shock data. The potential energy curves for He<sub>2</sub> and He<sub>2</sub><sup>+</sup> were determined using People's configuration-interaction method<sup>17</sup> and Dunning's correlation consistent polarized valence triple zeta basis set.<sup>18</sup> These potentials are plotted in Fig. 1.

The  $1\Sigma_g^+$  ground state of He<sub>2</sub> has the electron configuration  $(1\sigma_g^2 1\sigma_u^2)$  with no net bonding. The potential curve is basically repulsive except for weak long-range polarization forces. Analyses of highly accurate calculations<sup>19,20</sup> on the ground state of He<sub>2</sub> have shown that these forces give rise to a potential well of approximately 11 K. The He<sub>2</sub><sup>+</sup> molecular ion is formed by removing one electron from the  $\sigma_u$  anti-

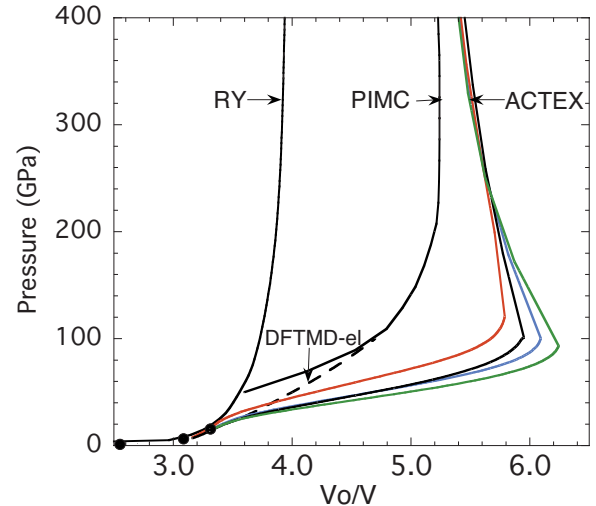


FIG. 2. (Color) Helium Hugoniot. Shock pressure versus compression  $V_0/V$ ,  $V_0=32.4 \text{ cm}^3/\text{mol}$ . Experimental measurements, Ref. 1 (filled circles). RY Hugoniot computed using soft-sphere fluid variational theory using He-He potential fitted to the principal Hugoniot (Ref. 2). PIMC (solid curve) and DFTMD-el (small dashed curve) calculations (Ref. 4). ACTEX Hugoniot from left to right: (a) He<sub>2</sub><sup>+</sup> with scattering states (red curve); (b) He<sub>2</sub><sup>+</sup> with bound and scattering states (black curve); (c) omitting He<sub>2</sub><sup>+</sup> bound and scattering states (blue curve); (d) He<sub>2</sub><sup>+</sup> with bound states (green curve).

bonding orbital of the ground state of He<sub>2</sub>, giving the  $X^2\Sigma_u^+$ , the bound He<sub>2</sub><sup>+</sup> state with the electron configuration  $(1\sigma_g^2 1\sigma_u)$ . The net number of bonding electrons leads to a binding energy<sup>16</sup> of 2.474 eV relative to the He<sup>+</sup>(1s) + He(1s<sup>2</sup>) dissociation limit. The  $X^2\Sigma_u^+$  potential energy curve in Fig. 1 has a well depth of 2.44 eV in good overall agreement with previous calculations.<sup>20,21</sup> The first excited state of He<sub>2</sub><sup>+</sup>,  $A^2\Sigma_u^+$ , has the configuration  $(1\sigma_g 1\sigma_u^2)$  with a net number of antibonding electrons. Consequently, the potential energy curve is repulsive at the internuclear separations shown in Fig. 1. Bagawan and Davidson<sup>22</sup> have shown that this state undergoes a curve crossing with the  $C^2\Sigma_g^+$  excited state at an internuclear distance of 0.767 Å. This state was not included in the Hugoniot calculations. It is beyond the scope of our present effort to include all of the excited species such as He-He\* possibly present, but if included they would likely reinforce the predictions of a large compression by absorbing more shock kinetic energy and constraining the temperature rise. In a fashion similar to that described in Ref. 14, we reorganized the activity equations in terms of the activities of electrons He<sup>2+</sup>, He<sup>+</sup>, He, and He<sub>2</sub><sup>+</sup>.

### III. RESULTS

Plotted in Fig. 2 are the results of the present ACTEX calculations: the Hugoniot measurements of Nellis *et al.*,<sup>1</sup> earlier calculations by RY,<sup>2</sup> and the recent PIMC simulations of Militzer.<sup>4</sup> The RY Hugoniot, which was computed using only the He-He potential increases smoothly and reaches its maximum compression at the ideal gas limit of  $V_0/V=4$ . The

PIMC simulations<sup>4</sup> predict a Hugoniot with a maximum compression near 5.24-fold at a pressure of 360 GPa and 150 000 K ( $kT=12.93$  eV). But the PIMC Hugoniot does not converge to the experimental shock measurements. Instead, a convergence of theory with experiment is achieved by employing a DFTMD simulation with electronic excitations added on (DFTMD-el).

As discussed above, the ACTEX calculations include higher-order plasma corrections, but are currently limited to second virial corrections for repulsive interactions that occur at low temperature. The lowest temperature considered along the Hugoniot in the present work is about 4000 K, where neutral helium is the main contributor and  $PV/nkT$  is 1.45 at 15 000 K. At these values of  $PV/nkT$ , the second virial term is dominant. The third virial term would make a small contribution and has been neglected. In the case of deuterium, considered in Ref. 8,  $PV/nkT$  is somewhat larger.

In the present study, four sets of ACTEX Hugoniot calculations were made, each with a different combination of bound and scattering states, the purpose being to gather insight into the influence that different interactions play in shaping the Hugoniot. All four sets of calculations included the He-He ground state, thermal electronic excitations, and ionization and connected smoothly to the gas gun shock measurements near 16 GPa. The most physically correct of the ACTEX calculations, the “full model” (black curve) includes both the bound  $\text{He}_2^+ X^2\Sigma_u^+$  and  $A^2\Sigma_g^+$  scattering state interactions. This Hugoniot softens with increasing pressure, reaching a maximum compression near of 5.95-fold at a pressure of 100 GPa and a temperature of 53 000 K ( $kT=4.57$  eV). Above 360 GPa, the PIMC and ACTEX results begin to converge, and with increasing pressure and temperature approach the fourfold compression limit of an ideal gas plasma.

The Hugoniot that includes the bound state  $X^2\Sigma_u^+$  but omits the scattering state  $A^2\Sigma_g^+$  (green curve) leads to an increase in the maximum compression relative to the full model. Omitting the bound state and keeping just the repulsive scattering state gives the least compression (red curve). In a fourth calculation, both bound and scattered states are omitted. This leads to some cancellation, but is shifted toward higher compression than if bound and scattering states are included. The reason is that, while the bound state  $X^2\Sigma_u^+$  is attractive and pushes to greater compression, and the repulsive scattering state  $A^2\Sigma_g^+$  pushes to less compression, dropping both states creates more compression due to the removal of the more repulsive scattered state. The calculated temperatures are plotted in Fig. 3. Surprisingly, the nearly linear relationship is virtually the same for PIMC, DFTMD-el,<sup>4</sup> and all four ACTEX calculations. The RY temperatures are the highest at all the pressures due to the absence of any thermal excitations. ACTEX was not used to calculate the second shock point of Nellis *et al.*<sup>1</sup> at 56 GPa. This point, which has a large uncertainty, had been calculated in the earlier report<sup>2</sup> by RY employing soft-sphere fluid theory and using only the He-He potential. Some insight into the physical changes occurring along the Hugoniot may be drawn from an examination of the species concentration shown in Fig. 4. Starting from the liquid, and up to 15.6 GPa, the gas gun experiments show no evidence for

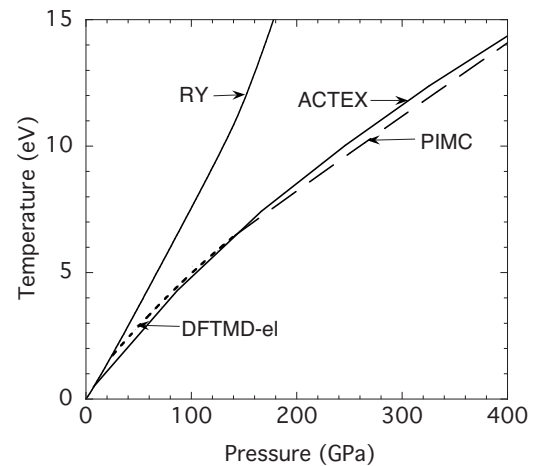


FIG. 3. Calculated helium shock temperatures versus compression. PIMC and DFTMD-el results were taken from Ref. 4. The ACTEX Hugoniot temperature calculations include  $\text{He}_2^+$  bound and scattering states (solid curve).

electronic excitation. This is consistent with our calculations, which show that, starting near and above 20 GPa, thermal excitation initiates formation of the low-lying  $X^2\Sigma_u^+$ , the bound  $\text{He}_2^+$ , and the  $A^2\Sigma_g^+$  scattering states. Near 60 GPa, the  $X^2\Sigma_u^+$   $\text{He}_2^+$  species reaches its maximum concentration at about 20%. The  $\text{He}^+$  concentration up to this pressure is mostly associated with the scattering state and is also near 20%. With increasing pressure the concentration of bound  $\text{He}_2^+$  decreases while the fractions of  $\text{He}^+$  and  $\text{He}^{2+}$  increase due to  $K$ -shell ionization.

Over the entire pressure range, the repulsive fraction of He atoms steadily decreases and the total fraction of ions increases. The two curves cross near 170 GPa. Above this pressure, the system becomes increasingly dominated by the dense plasma phase. It is arguable that the crossing near 170 GPa is related to the maximum compression predicted to occur near 100 GPa. Since the PIMC calculations predict a maximum compression near 360 GPa, a scaling argument would predict that the atom and ion curves cross near 500 GPa and that ionization increases less rapidly with pres-

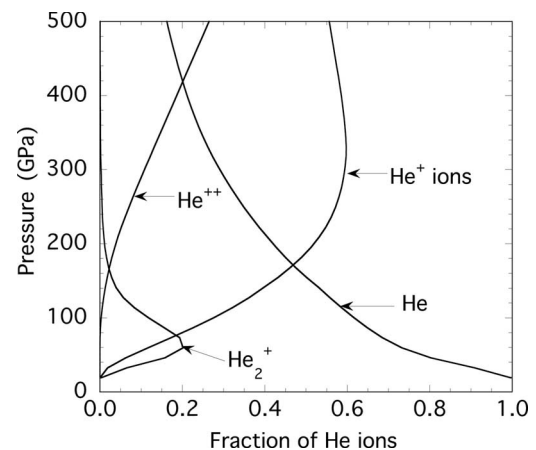


FIG. 4. Concentration of species (indicated) calculated along the ACTEX He Hugoniot, plotted in terms of ion fraction and pressure.

sure in the PIMC calculations than by ACTEX. In order to obtain a better understanding for the origin of these differences, it is necessary to have knowledge of the species fractions present along the PIMC Hugoniot.

#### IV. DISCUSSION

To some extent, the interest in the shock compression of liquid He stems from the controversy, regarding shock-compressed liquid deuterium (where the maximum compression measured experimentally and predicted theoretically), which lies over a wide compression range from 4.3-fold (Ref. 23) to near six-fold.<sup>24,25</sup> For the case of D<sub>2</sub>, a PIMC calculation predicts a maximum compression near 4.2-fold (Ref. 26) and for He near 5.24-fold,<sup>4</sup> while ACTEX consistently predicts maximum compressions nearer six-fold.<sup>8</sup>

In the case of He, thermal electron excitation is the dominant mode of change along the Hugoniot, in contrast to D<sub>2</sub>

where it is molecular dissociation, making any casual comparisons likely to be deceptive. However, considering the relative simplicity of the He atom and the fact that four variations of the present model made only relatively small differences in the Hugoniot, it is likely that theoretical predictions of the maximum compression for He will be more reliable than for D<sub>2</sub>. For example, the He predictions of PIMC (5.24-fold) and ACTEX (5.95-fold) calculations average to a maximum compression of 5.6 and are in better agreement than for the case of D<sub>2</sub>.

#### ACKNOWLEDGMENTS

The work presented here was partially supported under the auspices of the U.S. Department of Energy by the University of California Lawrence Livermore National Laboratory under Contract No. W-7405-ENG-48.

- 
- <sup>1</sup>W. J. Nellis, N. C. Holmes, A. C. Mitchell, R. J. Trainor, G. K. Governo, M. Ross, and D. A. Young, *Phys. Rev. Lett.* **53**, 1248 (1984).
- <sup>2</sup>M. Ross and D. A. Young, *Phys. Lett. A* **118**, 463 (1986).
- <sup>3</sup>J. M. Aparicio and G. Chabrier, *Phys. Rev. E* **50**, 4948 (1994); C. Winisdoerffer and G. Chabrier, *ibid.* **71**, 026402 (2005).
- <sup>4</sup>B. Militzer, *Phys. Rev. Lett.* **97**, 175501 (2006).
- <sup>5</sup>B. A. Remington, P. R. Drake, and D. D. Ryutov, *Rev. Mod. Phys.* **78**, 755 (2006).
- <sup>6</sup>F. J. Rogers, *Phys. Rev. A* **10**, 2441 (1974).
- <sup>7</sup>F. J. Rogers, in *High Pressure Equations of State: Theory and Applications*, edited by S. Eliezer and R. A. Ricci (North-Holland, New York, 1991).
- <sup>8</sup>F. J. Rogers, *Contrib. Plasma Phys.* **43**, 355 (2003); **41**, 179 (2001).
- <sup>9</sup>F. J. Rogers, *Phys. Rev. A* **23**, 1008 (1981).
- <sup>10</sup>F. J. Rogers, *Phys. Rev. A* **24**, 1531 (1981).
- <sup>11</sup>R. Abe, *Prog. Theor. Phys.* **22**, 213 (1959).
- <sup>12</sup>M. S. Cooper and H. E. DeWitt, *Phys. Rev. A* **8**, 1910 (1973).
- <sup>13</sup>J. E. Mayer and M. G. Mayer, *Statistical Mechanics* (John Wiley, New York, 1940).
- <sup>14</sup>F. J. Rogers and A. Nayfonov, *Astrophys. J.* **576**, 1064 (2002).
- <sup>15</sup>J. N. Bardsley, *Phys. Rev. A* **3**, 1317 (1971).
- <sup>16</sup>R. J. Blint, *Phys. Rev. A* **14**, 2055 (1976).
- <sup>17</sup>J. A. Pople, M. Head-Gordon, and K. J. Raghavachari, *Chem. Phys.* **87**, 5968 (1987).
- <sup>18</sup>T. H. Dunning, Jr., *J. Chem. Phys.* **90**, 1007 (1989).
- <sup>19</sup>R. A. Aziz and M. J. Slaman, *J. Chem. Phys.* **94**, 8047 (1991).
- <sup>20</sup>A. R. Janzen and M. J. Slaman, *J. Chem. Phys.* **103**, 9626 (1995).
- <sup>21</sup>W. Cencek and J. Rychlewski, *J. Chem. Phys.* **102**, 2533 (1995).
- <sup>22</sup>A. D. O. Bawagan and E. R. Davidson, *Chem. Phys. Lett.* **266**, 499 (1997).
- <sup>23</sup>L. B. Da Silva, P. Celliers, G. W. Collins, K. S. Budil, N. C. Holmes, T. W. Barbee, Jr., B. A. Hammel, J. D. Kilkenny, R. J. Wallace, M. Ross, R. Cauble, A. Ng, and G. Chiu, *Phys. Rev. Lett.* **78**, 483 (1997).
- <sup>24</sup>M. D. Knudson, D. L. Hanson, J. E. Bailey, C. A. Hall, J. R. Asay, and C. Deeney, *Phys. Rev. B* **69**, 144209 (2004).
- <sup>25</sup>G. V. Boriskov, A. I. Bykov, R. Il'kaev, V. D. Selemir, G. V. Simakov, R. F. Trunin, V. D. Urlin, A. N. Shuikin, and W. J. Nellis, *Phys. Rev. B* **71**, 092104 (2005).
- <sup>26</sup>B. Militzer and D. M. Ceperley, *Phys. Rev. Lett.* **85**, 1890 (2000).